

# Evaluation of effective stress times and stress levels from mission profiles for semiconductor reliability



A. Hirler<sup>a,\*</sup>, J. Biba<sup>a</sup>, A. Alsioufy<sup>a,b</sup>, T. Lehndorff<sup>a,b</sup>, T. Sulima<sup>a</sup>, H. Lochner<sup>b</sup>, U. Abelein<sup>c</sup>, W. Hansch<sup>a</sup>

<sup>a</sup> Universität der Bundeswehr München, Werner-Heisenberg-Weg 39, 85577 Neubiberg, Germany

<sup>b</sup> AUDI AG, Auto-Union-Straße 1, 85045 Ingolstadt, Germany

<sup>c</sup> Infineon Technologies AG, Am Campeon 1-12, 85579 Neubiberg, Germany

## ARTICLE INFO

### Article history:

Received 19 May 2017

Received in revised form 12 June 2017

Accepted 13 June 2017

Available online 21 June 2017

### Keywords:

Automotive electronics

Mission profile

Semiconductor reliability

Cumulative stress modeling

Effective stress

## ABSTRACT

Lifetime and duty cycles of automotive electronics are increasing, inducing new challenges to reliability predictions and testing. For qualification purposes, the automotive industry generates various time-dependent mission profiles with various stressors and varying stress levels according to different use cases.

We present a theoretical model, describing the common approach, to reduce the stressors from time-dependent mission profiles to the two single parameters “effective stress level” and “effective stress time” for equivalent reliability testing. In a first step, the cumulative exposure (CE) model is shown to describe the future reliability behaviour after steplike stress level changes. Taking into account the individual characteristic lifetimes  $T_{63}$  of the corresponding Weibull distributions, in a second step, an effective  $T_{63}$  lifetime can be derived. For this calculation, periodic stress cycles are defined and transformed into an equivalent effective stress level. This procedure confirms the industry-wide used approach of dealing with effective stress levels for reliability testing.

For the experimental validation metal-oxide-semiconductor (MOS) capacitors are fabricated and stressed by voltage and temperature. The received reliability data fit the theoretical predictions within the statistical variations.

© 2017 Elsevier Ltd. All rights reserved.

## 1. Introduction

The automotive industry is steering into a future of new, innovative challenges with driver assistance systems, autonomous driving, electric mobility and car connectivity on their way into the market. In order to realise such ambitious new features, the usage of leading-edge semiconductor technologies is essential. To further on secure the typical high reliability standards requested in the automotive industry, great efforts are made to standardise and advance existing qualification processes. One example are the stress test qualification plans of the Automotive Electronics Council (AEC). In addition to standardised test conditions, they also consider customer mission profile based qualification and robustness validation in case the standard conditions in the AEC-Q100 are not sufficient to cover the application's lifetime requirements [1].

Mission profiles are usually a conglomeration of all relevant stresses on the chosen product in form of time series, histograms or effective

stressors (see Fig. 1). Due to the extended duty cycles e.g. for electric mobility applications that are predicted for the future, standard test times may not be sufficient anymore and other ways of qualification must be considered. Either a thorough robustness validation [2] is performed or the already hastened qualification test must be further accelerated. The latter is not always possible, because at higher stresses other usually insignificant failure mechanisms can become the dominant reason for failure or other components of the test device will fail due to enhanced stresses, for instance packaging at high temperatures. Besides that, the degree of detail of mission profiles is constantly increasing to distinguish e.g. different installation locations or supplier adjustments.

While the use of mission profiles becomes increasingly necessary, as already stated, literature on the physical justification for the creation of histograms and effective qualification stresses is barely available.

Therefore, a basic concept is presented on this issue with focus on the experimental validation of cumulative damage models as well as the transformation of alternating step-stress accelerated life tests (SSALT) into one parameter equivalents of effective stress level and effective stress time. The experimental validation is done by using

\* Corresponding author.

E-mail address: [alexander.hirler@unibw.de](mailto:alexander.hirler@unibw.de) (A. Hirler).

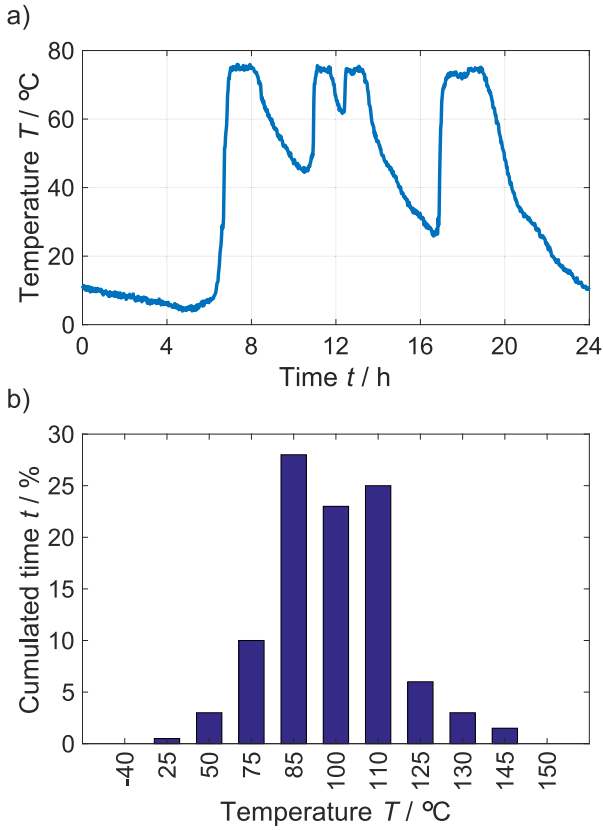


**Fig. 1.** Mission profiles a) an exemplary stress-time diagram; b) an exemplary stress histogram.

metal-oxide-semiconductor (MOS) capacitors and their failure mechanism time-dependent dielectric breakdown (TDDB) [3] for testing purposes.

## 2. Cumulative damage model

In order to analyse accelerated life test data from step-stress tests, different cumulative damage models were proposed in literature [4,5,6]. It was shown that for specific conditions these different models coincide with each other [7]. As it is the case for the presented data, Weibull distributions with a shape parameter  $\beta$  of slightly  $> 1$  are not suitable to expose the differences of the mentioned models.

Nelson [4] suggested the cumulative exposure (CE) model. While he applied his model to Weibull distributions and an inverse power law stress-lifetime relationship, the CE model can be generalised [8] and applied to many other accelerated life models.

Nelson stated that the remaining life of a specimen depends only on the current cumulative fraction failed and the cumulative distribution function (CDF) of the current stress. The order in which the stress is accumulated is irrelevant and consequently the CE model is a linear one [4].

### 2.1. Theoretical model description

The CE model can be described by starting with two Weibull CDFs  $F_1(t)$  and  $F_2(t)$ . The resulting CDF  $F_{CE}(t)$  depends on the time  $t$  and the point of time  $t_i$ , when the stress level  $i$  is applied:

$$F_{CE}(t) = F_1(t), \quad t_1 < t \leq t_2, \quad (1)$$

$$F_{CE}(t) = F_2(t - t_2 + t_2'), \quad t > t_2. \quad (2)$$

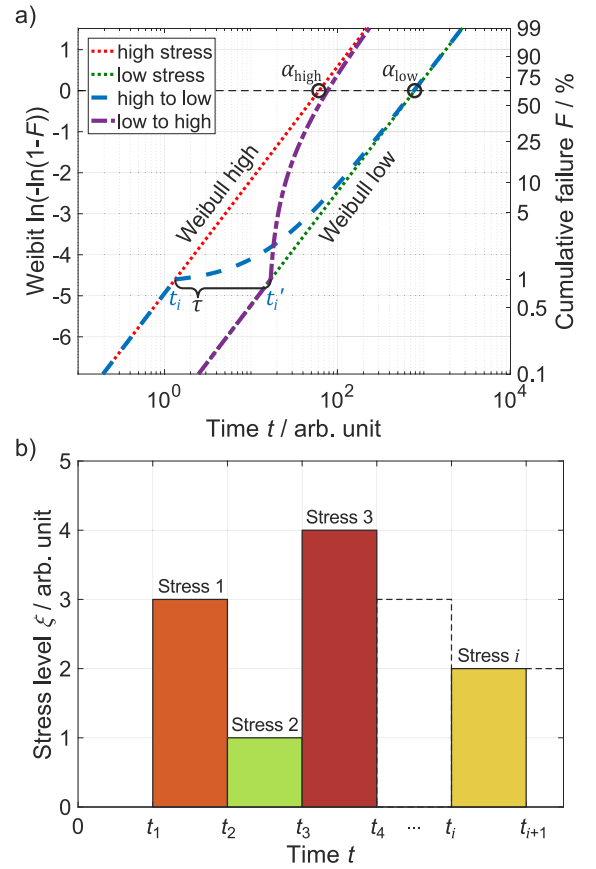


**Fig. 2.** a) Weibull CDFs of step-stress life tests according to the CE model with two different stress levels and their permutation are drawn with dashed lines, whereas the constant reference stresses are drawn with dotted lines. b) Arbitrary mission profile consisting of various step stresses.

$t_2'$  indicates the equivalent start time of the second CDF  $F_2(t)$ . This is when the cumulative fractions of  $F_1(t_2)$  and  $F_2(t_2')$  have the same value (see Fig. 2a). With the introduction of an additional location parameter  $\tau_i$  of the Weibull distribution,

$$\tau_i = t_i - t_i', \quad (3)$$

the current CDF of step  $i$  can be simplistically described as a three-parametric Weibull distribution. The CDF is given by

$$F_i(t) = 1 - \exp \left[ - \left( \frac{t - \tau_i}{\alpha_i} \right)^\beta \right], \quad (4)$$

where  $\alpha_i$  is the Weibull scale parameter, which corresponds to the  $T_{63}$  time, and  $\beta$  denotes the Weibull shape parameter.

When considering the arbitrary mission profile in Fig. 2b with stress change times  $t_i$ , where  $t_1' = 0$ , the CDFs of the CE model  $F_{CE}(t)$  can recursively be expressed as the following:

$$F_{CE}(t) = F_1(t - \tau_1), \quad t_1 < t \leq t_2, \quad (5)$$

$$F_{CE}(t) = F_2(t - \tau_1 - \tau_2), \quad t_2 < t \leq t_3, \quad (6)$$

$$F_{CE}(t) = F_3(t - \tau_1 - \tau_2 - \tau_3), \quad t_3 < t \leq t_4, \quad (7)$$

$$F_{CE}(t) = F_i \left( t - \sum_{k=1}^i \tau_k \right), \quad t_i < t \leq t_{i+1}. \quad (8)$$

From this algorithm and Fig. 2b it is obvious that if several stress levels are repeated, these levels can be summed up to a histogram as shown in Fig. 1b.

## 2.2. Empirical validation of the CE model

For the purpose of verifying the statements drawn from the CE model, SSALT measurements were performed on MOS capacitors fabricated on 4"-wafers in our semiconductor cleanroom. These ultrathin (2.7 nm) SiO<sub>2</sub> dielectric capacitors have a square shape with a length of 100 μm. The failure mechanism of TDDB was investigated in accumulation mode with voltage and temperature as variable stressors. The reliability measurements were performed with the semiconductor analyser Keysight B1500A in constant voltage mode. Prior to the stress measurement for each diode the leakage current was checked at 1.0 V to ensure the integrity of the oxide. The failure criterion for the MOS capacitors is a hard breakdown in form of a local current jump of at least 1 μA at a sampling rate of 10 Hz. After the investigation of every individual current-time characteristic the breakdowns are cumulated and plotted against time in a Weibull probability diagram. The results of voltage and temperature stress are presented in Fig. 3.

The voltage stress measurements were conducted at room temperature. For low stress a voltage of 2.5 V, for high stress a voltage of 2.7 V was chosen. First, the stress time until the change point was arbitrarily chosen to be  $T_{50}$ , which denotes the median time of the failure distribution, 569 s for low and 45 s for high stress, taken from the experiment. Then the constant stress level is changed to either a higher or lower stress level and then hold until the last failure percentile is reached.

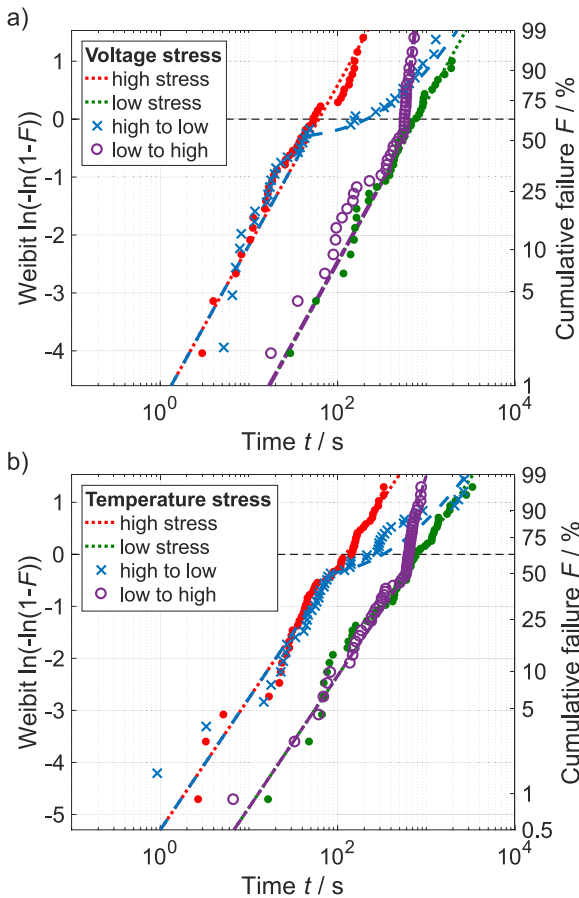


Fig. 3. Breakdown distributions of MOS capacitors in analogy to Fig. 2 for both stress level permutations with the stress changed at the median time  $T_{50}$ . Crosses indicate the step sequence from high to low stress levels and open circles the vice versa sequence for a) voltage and b) temperature stress.

The failure times of the specimens follow the exact behaviour of the previously calculated three-parametric Weibull distributions with respect to the statistical variation. The location parameter  $\tau$  in this example is the difference of both  $T_{50}$  times, which is  $\pm 524$  s respectively.

For the temperature stress measurements at a constant voltage of 2.4 V the two stress levels were chosen to be 50 °C and 80 °C. The median times  $T_{50}$  are respectively 587 s and 90 s. Therefore, the location parameter  $\tau$  is derived as  $\pm 497$  s.

The presented approach is also valid in case of three or more different stress levels, which has been experimentally reproduced as well, but is not presented here. If failure mechanisms with self-healing abilities or simultaneously acting stressors are investigated, a modified CE model must be used.

## 3. Deduction of effective stress levels and effective stress times

The CE model transformation of a time series into an equivalent stress histogram has been proven applicable to the used experimental setup. The representation of a mission profile as such a stress histogram can also be interpreted as a step-stress function.

From this basis onward, an evaluation of the step function and mission profile cycles enables the transformation of a steplike mission profile into an approximate equivalent representation in form of an effective constant stress.

### 3.1. Transformation of a histogram to effective stress

The main premise of the following approach is: if the stress level is changed, the failure mechanism and the Weibull shape parameter  $\beta$  stay constant. Therefore, the acceleration factor AF between two arbitrary stresses  $i$  and  $j$  can be expressed as:

$$AF_{[i;j]} = \frac{\alpha_j}{\alpha_i} \quad (9)$$

If an alternating steplike mission profile is assumed, the Weibull CDFs of all possible permutations intersect at every full mission profile cycle. For these points of intersection an effective constant stress distribution, characterised by the calculated effective scale parameter  $\alpha_{\text{eff}}$ , can be derived:

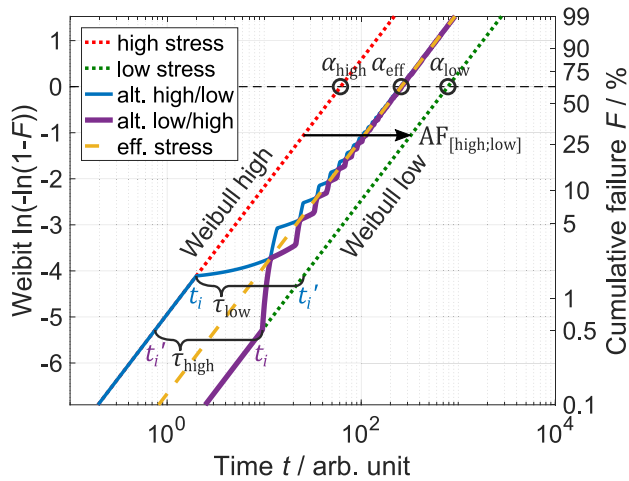
$$\frac{\alpha_{\text{eff}}}{\sum_{i=1}^n t_i} = \frac{\alpha_j}{\sum_{i=1}^n t_i AF_{[i;j]}} \quad (10)$$

Fig. 4 illustrates this behaviour without loss of generality, for a simple, alternating, two-step mission profile. It is easy to see that the deviation of the alternating step-stress distributions from the calculated effective stress equivalent decreases as more mission profile cycles are completed. The first failure in an automotive application is usually expected after a duration which is a few orders of magnitudes longer than the completion time of a one-day mission profile cycle, for instance. The starting alternating failure rates would not be observed in this case.

### 3.2. Exposition with experimental data

The combined CDF of the alternating SSALT is calculated with the recursive formulation of the CE model (see Eq. (8)). For that, the stress times for every stress level were arbitrarily chosen on the basis of previous reference constant stress measurements. In our case, the lower stress at 2.5 V has an  $\alpha$  of 782 s and a chosen dwell time of 9.6 s and the higher stress at 2.7 V has an  $\alpha$  of 61 s and a chosen dwell time of 2 s. The experimental breakdown data follows the anticipated CDF behaviour as expected (see Fig. 5). In addition, individual steps are visible.

The effective stress to match the alternating stress levels was calculated with Eq. (10). In this case, the computed  $\alpha_{\text{eff}}$  is 257 s which



**Fig. 4.** Different alternating stress levels (solid lines) approach a constant effective stress failure distribution (dashed line) as more cycles are completed.

corresponds to a stress level of 2.58 V. The data of the effective constant stress level fit well to the alternating step-stress measurement. This demonstrates the effectivity of the presented model. In addition, it can be seen, that both realisations of the initial mission profile histogram become less distinguishable as the number of full step-stress cycles increases.

### 3.3. From effective stresses to reliability test times

In a first step, the mission profile histogram is transformed into an effective stress level. The calculated stress time should represent the expected lifetime of the vehicle. To extrapolate the reliability testing to longer vehicle lifetimes the necessary longer testing times may not be practical. Therefore, if the test time cannot easily be expanded, in a second step, the effective stress level for the entire lifetime has to be transformed into a higher test stress level. This can be performed if the underlying stress-lifetime relationship of the observed failure mechanism is known for all stress levels and no additional distortions are activated.

## 4. Conclusion

The demonstrated CE model for approaching cumulative damage distributions is shown to be applicable and the empirical validity was demonstrated for two stressors, voltage and temperature.

By the means of the CE model, an original time-dependent stress profile can be transformed into a condensed stress histogram, which is a frequently used representation of mission profiles in the automotive industry.

The histogram can then be transformed into an effective stress level. As stated particularly for automotive applications, at the time of first failure the actual stress distribution already matches the one for the determined effective stress level. That means, alternating failure rates will not be observed.

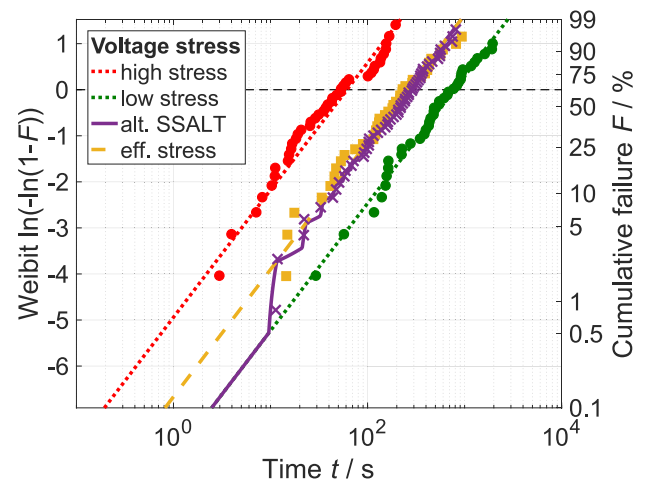


**Fig. 5.** Breakdown distributions of MOS capacitors in analogy to Fig. 4. An alternating voltage step-stress function, beginning with the lower of two constant stress levels (filled circles), is depicted with crosses and a solid line. The effective constant stress failure distribution with filled squares overlaps nearly completely with the step-stress distribution.

An accelerated life test with a higher constant stress level and a shortened effective stress time can therefore be developed and a reliability qualification or robustness validation can be performed on that basis.

## Acknowledgements

This contribution is funded as part of the autoSWIFT project (project label 16ES03) within the research program ICT 2020 by the German Federal Ministry of Education and Research (BMBF).

## References

- [1] Automotive Electronics Council (AEC), Failure mechanism based stress test qualification for integrated circuits, AEC - Q100 - REV-H, 2014.
- [2] W. Kanert, Robustness validation – a physics of failure based approach to qualification, *Microelectron. Reliab.* 54 (2014) 1648–1654, <http://dx.doi.org/10.1016/j.microrel.2014.07.010>.
- [3] J.W. McPherson, Time dependent dielectric breakdown physics – models revisited, *Microelectron. Reliab.* 52 (2012) 1753–1760, <http://dx.doi.org/10.1016/j.microrel.2012.06.007>.
- [4] W. Nelson, Accelerated life testing – step-stress models and data analyses, *IEEE Trans. Reliab.* R-29 (1980) 103–108, <http://dx.doi.org/10.1109/TR.1980.5220742>.
- [5] M.H. DeGroot, P.K. Goel, Bayesian estimation and optimal designs in partially accelerated life testing, *Nav. Res. Logist. Q* 26 (1979) 223–235, <http://dx.doi.org/10.1002/nav.3800260204>.
- [6] G.K. Bhattacharyya, Z. Soejoeti, A tampered failure rate model for step-stress accelerated life test, *Commun. Stat. Theory Methods* 18 (1989) 1627–1643, <http://dx.doi.org/10.1080/03610928908829990>.
- [7] R. Wang, H. Fei, Conditions for the coincidence of the TFR, TRV and CE models, *Stat. Pap.* 45 (2004) 393–412, <http://dx.doi.org/10.1007/BF02777579>.
- [8] W. Zhao, E.A. Elsayed, A general accelerated life model for step-stress testing, *IIE Trans.* 37 (2005) 1059–1069, <http://dx.doi.org/10.1080/07408170500232396>.